Ore Geology Reviews 154 (2023) 105336

Contents lists available at ScienceDirect

Ore Geology Reviews

journal homepage: www.elsevier.com/locate/oregeorev

Evidence of rare earth elements origin in acid mine drainage from the Iberian Pyrite Belt (SW Spain)

Rafael León [a,*], Francisco Macías [a], Carlos R. Cánovas [a], Ricardo Millán-Becerro [a], Rafael Pérez-López [a], Carlos Ayora [b], José Miguel Nieto [a]

[a] Department of Earth Sciences and Research Center on Natural Resources, Health and the Environment, University of Huelva, Campus "El Carmen", E-21071 Huelva, Spain

[b] Institute of Environmental Assessment and Water Research (IDAEA-CSIC), Jordi Girona 18, 08034 Barcelona, Spain

ARTICLE INFO

Keywords:
Poderosa mine
Perrunal mine
Acid leachates
Monazite
Xenotime
Parisite

ABSTRACT

Acid mine drainage (AMD) is a worldwide pollution problem of watersheds. In addition to toxic metal(oid)s and acidity, many elements of economic interest are released into the environment, which make AMD a potential strategic secondary source of these elements such as rare earth elements (REE). Despite the importance of these metals, their origin in AMD is still uncertain. Recent hypotheses suggest preferential leaching of REE-enriched minerals as a possible source. Leaching tests with H_2SO_4 have been developed to simulate the interaction under AMD formation conditions with sulfide bodies and host rocks from two representative mining areas in the Iberian Pyrite Belt: the Perrunal and Poderosa mines (SW of Spain). The REE patterns and Ce and Eu anomalies of the rock leachates have confirmed the geochemical relationship between the AMD and certain country rocks (felsic and mafic volcanics, and shales). A detailed chemical and mineralogical study has confirmed the existence of a diversity of minerals with high concentrations of REE. Thus, the minerals with the highest REE contents are also those with the fast dissolution kinetics under acid conditions: REE phosphates (monazite and xenotime type) and carbonates (parisite type). Finally, petrographic evidence of the selective leaching of these minerals clearly supports these minerals as the main source of REE in the AMD.

1. Introduction

The mismanagement of large volumes of sulfide-rich wastes generated during the metal and coal mining may result in the oxidation of sulfides when exposed to oxygen and water (Johnson and Hallberg, 2005; Nordstrom et al., 2015). This result, known as Acid Mine Drainage (AMD), generates a leachate that commonly releases a large amount of metal(oid)s, sulfates, and acidity to streams and groundwater, which is of great concern worldwide (Akcil and Koldas, 2006) due to its longevity (Younger, 1997). In addition to these pollutants, AMD may have high concentrations of other elements of economic interest such as the rare earth elements (REE). These elements, which include Lanthanides (La-Lu) together with other geochemically related elements such as Sc and Y, have properties that make them essential components for applications in technology (e.g., permanent magnets, catalysts, batteries, electronic devices or LED lighting), as well as in the nuclear, military, aerospace, and medical sectors (Hatch, 2012; Lucas et al., 2014). This large number of applications has generated a growing demand, which in some cases is not sufficiently supplied by primary deposits. This primary supply risk has promoted the search for secondary sources of these elements as a priority strategy worldwide (Binnemans et al., 2013). In this sense, numerous recent works have studied the viability of AMD from metal and coal mines as a strategic secondary source of REE (e.g., Ayora et al., 2016; Ziemkiewicz et al., 2016; Macías et al., 2017; Stewart et al., 2017; Zhang and Honaker, 2018, 2020; Vass et al., 2019; Hedin et al., 2020; León et al., 2021). As mentioned above, part of the interest of these elements is due to their high concentrations in AMD, between hundreds to thousands of μg/L (Ayora et al., 2016), several orders of magnitude above the concentrations found in natural waters, which are usually below tens of μg/L (Noack et al., 2014). Although AMD is relatively enriched in middle REE (MREE; from Eu to Dy) when normalized to crustal values, it has a high variability in the enrichment of light REE (LREE; from La to Sm) and heavy REE (HREE; from Ho to Lu), which can determine both its economic potential and its possibilities of valorization (León et al., 2021).

The MREE enrichment has been widely shown in AMD from sulfide

* Corresponding author.
E-mail address: Rafael.leon@dct.uhu.es (R. León).

https://doi.org/10.1016/j.oregeorev.2023.105336
Received 28 June 2022; Received in revised form 21 November 2022; Accepted 2 February 2023
Available online 7 February 2023

and coal mining areas (Verplanck et al., 2001; Da Silva et al., 2009; Pérez-López et al., 2010; Sahoo et al., 2012; Ayora et al., 2016). Although the fractionation processes of REE in low pH systems have been extensively studied, the source of the rare earths and this MREE enrichment in AMD is still uncertain. According to Welch et al. (2009), the REE pattern could be strongly controlled by the Fe-cycle. During jarosite precipitation, a depletion of LREE in the pore water is observed, being retained in the solid phase. The subsequent transformation of jarosite to goethite, with a preferential sorption capacity of HREE (Verplanck et al., 2004; Olías et al., 2005) would additionally cause the depletion of HREE in the pore water, leaving a MREE enriched pattern. However, other authors suggest different hypotheses such as mobilization of MREE by complexation of sulfite or other sulfur species during pyrite oxidation (Grawunder et al., 2014), existence of REE partitioning in the colloidal fraction (Åström and Corin, 2003), exchange surface reactions with clays, Fe/Mn oxides or Fe/Al oxyhydroxides (Leybourne et al., 2000; Serrano et al., 2000; Åström, 2001; Coppin et al., 2002; Gammons et al., 2005; Lozano et al., 2019a, 2019b, 2020a, 2020b; Liu et al., 2022), differences in behavior of each REE during complexation with sulfates and to a lesser extent carbonates and phosphates (Möller and Bau, 1993; Sholkovitz, 1995; Tang and Johannesson, 2003; Zhao et al., 2007) or preferential leaching of MREE-enriched minerals (Johannesson and Zhou, 1999; Worrall and Pearson, 2001; Merten et al., 2005; Leybourne and Cousens, 2005; Sun et al., 2012). Recent Nd isotopic studies supported the latter hypothesis, suggesting preferential leaching of apatite or other MREE-enriched phosphate phases during water–rock interaction as the origin of REE in AMD (Wallrich et al., 2020).

Accordingly, our objective is focused on studying the behavior of REE during the water–rock interaction in AMD systems, as well as the mineralogical identification of potential REE-hosting minerals in the country rocks commonly found in these environments. In this sense, the Iberian Pyrite Belt (IPB), a large metallogenic polymetallic sulfide province located in the southwest of the Iberian Peninsula, with intense mining activity developed since antiquity, may be the appropriate location to study such processes. The intensity of sulfide oxidation and host rock dissolution processes for long periods has generated a big volume of mine waste that produces around 1 m^3/s of acidic water in the whole area during baseflow conditions. For this purpose, the Perrunal and Poderosa mines, both located in the northeast of the IPB, have been selected as study areas due to their contrasting geological and hydrogeochemical differences (Cánovas et al., 2016, 2018), which could be representative of the entire variability in AMD-forming setting that can be found in the IPB.

2. Materials and methods

2.1. Geological setting of the study areas

The high concentration of massive sulfide deposits in the IPB has led to its exploitation during the last 4,500 years (Nocete, 2006). Despite this long-lasting mining activity in the area, the most intensive exploitation period occurred since 1850, with the settlement of British consortia (Olías and Nieto, 2015). At the Poderosa mine, mining activity dates back at least to Roman times, with remains of some abandoned galleries (Cánovas et al., 2018). However, large-scale mining was developed from 1864 to 1924, during which around 0.6 Mt of sulfides were extracted (Gonzalo and Tarín, 1888; Pinedo Vara, 1963). Afterwards, only minor activities were carried out in this mine, especially obtaining Cu from AMD by cementation or recovering Au from gossan by heap-leaching cyanidation. Limited remediation measures occurred in 1990 after the cessation of these minor mining activities. There is also evidence of mining activity at the Perrunal mine from Tartessian and Roman times, however, intensive exploitation mainly took place from 1900 to 1968. In total, around 7.5 Mt of sulfides were extracted until 1960 through five underground galleries connected by wells (Pinedo Vara, 1963; Cánovas et al., 2016). After the cessation of mining activity in 1968, the underground system was flooded, leaving a ventilation tunnel as the only outlet for the AMD generated.

The two mine sites studied are located within the IPB, where sedimentary units of the Upper Paleozoic crop out interspersed by volcanic rocks and massive sulfide deposits. Stratigraphically the IPB can be divided into three units called, from botton to top, the Phyllite-Quartzite Group (PQ Group), the Volcano–Sedimentary Complex (VSC) and the Culm Group (Almodóvar et al., 2019). The PQ group consists of a thick alternation of shales and quartzites from the Upper Devonian (Moreno and Sáez, 1990). The VSC is a heterogeneous sequence of variable thickness that presents lateral wedging. The materials are of Upper Devonian-Lower Carboniferous in age and are composed of a volcanic sequence, where felsic and mafic episodes alternate, interspersed with a siliciclastic/volcanoclastic sedimentary sequence. In addition, there are deposits of chemical origin such as the siliceous cherts or jaspers, and the massive sulfides, which are formed mainly by pyrite, and lesser amounts of chalcopyrite, sphalerite, galena or arsenopyrite, among others. Finally, the Culm group is composed of shales, graywackes and conglomerates of Carboniferous age, resulting from synorogenic turbiditic deposition (Moreno, 1993). Eventually, all these materials underwent low-grade metamorphism during the Variscan orogeny.

The Poderosa mine area is mainly composed of materials belonging to the VSC, and to a lesser extent to the Culm Group (Fig. 1). The outcrop mainly consists of a thick sequence of epiclastic rocks of felsic composition (dacitic-rhyolitic), where the main mining activities (open pits and main galleries) were located. To the north of this sequence, a large formation of coherent rocks of rhyolitic composition can be found, which forms positive relief. To the south, there is a laterally discontinuous level of purple shales with radiolarians, characteristic of the hanging wall of the VSC, that also crop out in the vicinity of the open pits and galleries. The Culm group crops out in the southern part of the area as an alternation of gray shales and fine-grained sandstones. Manganese-rich jasper mineralization appeared both in lenses, causing small relief, and in smaller bodies within the VSC epiclastic units. Sulfides mainly appear as disseminated and small bodies in the rocks of the open pit, and toward the upper part of the section transformed into a gossan level. Finally, a secondary malachite mineralization appeared disseminated in the shales and epiclastic rocks of the open pit.

In the case of the Perrunal mine, again materials from the VSC and the Culm group crop out in the vicinity of the mining area (Fig. 2). To the north of the open pit, a sequence of felsic epiclastic rocks of the VSC appears. Among this thick series, there are some layers of volcanoclastic sandstones with fragments that have a larger grain size. In addition, a large lens of these sandstones appears between the open pit and the main gallery. Purple shales with radiolarians crop out as small lenses to the south and northeast of the open pit (Fig. 2). Manganese-rich jaspers appear both as small inclusions in the epiclastic rocks and in a large outcrop west of the open pit. Small sulfide lenses can also be found within the open pit. Dark gray shales and sandstones of the Culm group are widely represented to the south of the open pit and the main drainage gallery. Mafic volcanic rocks are found to the south of the sulfide mineralization (Pinedo Vara, 1963). These volcanics do not crop out in the mapped area, but have been observed in the same stratigraphic position to the east of the study area.

The tectonics of both mining areas is characterized by a series of thrusts striking in an approximate E-W direction that changes the position of the Culm and VSC-hanging wall shales, placing them below the epiclastic units that are stratigraphically located on the footwall. In addition, at least one major transform fault has been observed in the Poderosa mine area.

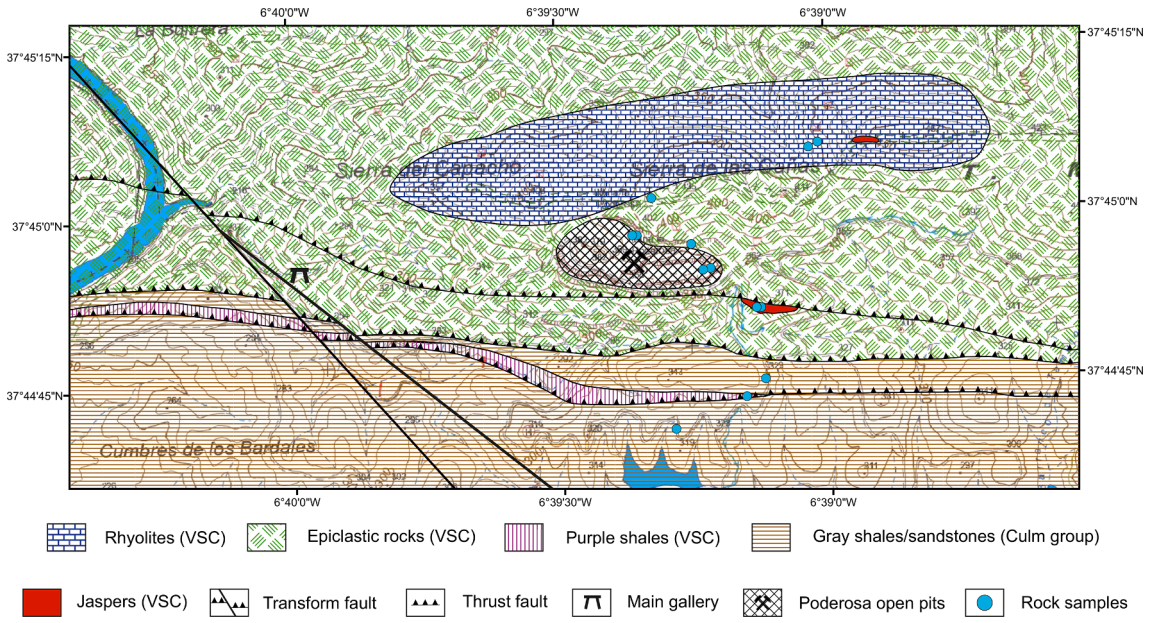

Fig. 1. Geological map of Poderosa mine area. A detailed view of the location of the rock samples collected in this area can be found in the KMZ file (Google Earth ™) available as electronic supplement.

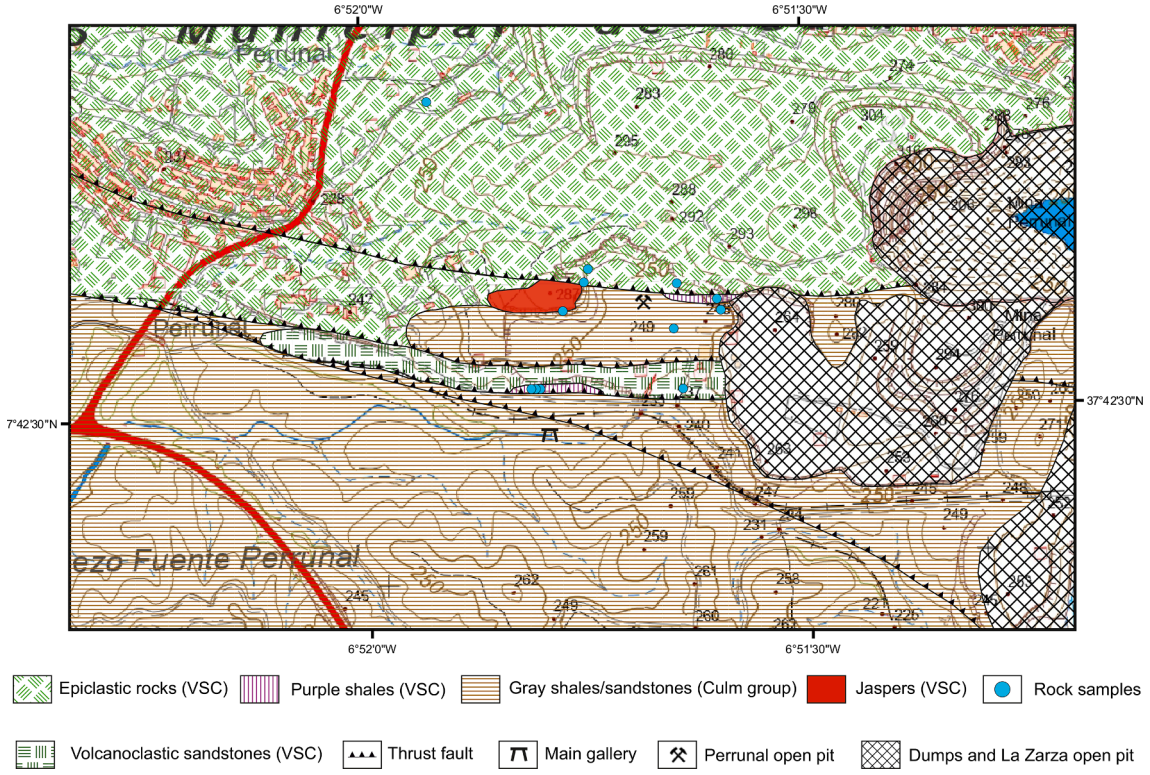

Fig. 2. Geological map of the Perrunal mine area. A detailed view of the location of the rock samples collected in this area can be found in the KMZ file (Google Earth ™) available as electronic supplement.

2.2. Data sampling, experiments and analysis

Firstly, 1:10.000 scale geological maps of the Poderosa and Perrunal mining areas were generated, and the representative lithologies were sampled in both areas (samples location can be seen on the KMZ file - Google Earth™ included as Supporting Information). The samples were examined under petrographic microscope and a JEOL JSM-IT500HR Field Emission Scanning Electron Microscope coupled with Oxford X-Max 150 Energy Dispersive System (FESEM-EDS), and a JEOL JXA-8200 SuperProbe Electron Probe Microanalyzer (EPMA) at the Research Services of the University of Huelva. The rest of the sample was powdered for chemical analysis and to perform leaching experiments. The concentration of major and trace elements was determined by Inductively Coupled Plasma-Atomic Emission Spectroscopy (ICP-AES) and Inductively Coupled Plasma-Mass Spectroscopy (ICP-MS), respectively, in the laboratories of SGS Canada Inc. Burnaby, after complete digestion of the

sample using the sodium peroxide fusion method. For the quality control of the method, blank samples, reference standards (OREAS681 and OREAS682) and duplicate analysis were used.

The leaching experiments consisted in batch sequential leaching tests with ultrapure reagents in a 1:40 sample-liquid mass ratio under agitation. Samples were first reacted with 1 N ammonium acetate in duplicate (two samples of 1 g for each lithology) for 4 h, to allow the removal of easily exchangeable cations, expected to be released only during the first contact with acidic water in the system (Stewart et al., 2001; Wallrich et al., 2020). After rinsing with ultrapure water, these samples were leached with 0.025 M and 0.05 M sulfuric acid for another 4 h, simulating the long-term interaction between AMD (with different grades of leaching capacity) and host rocks in mining districts (Wallrich et al., 2020). The solutions obtained in each step were filtered through < 0.2 μm cellulose nitrate filters prior analysis by ICP-OES and ICP-MS at the Research Services from the University of Huelva. Additionally, temporal datasets of AMD from Poderosa (n = 77) and Perrunal (n = 55) AMD leachates, collected between 2013 and 2017 and 2010–2017, respectively, together with some other main sources of AMD (n = 100) in the IPB (León et al., 2021) were considered in this study.

To analyze potential REE fractionation processes, concentrations have been normalized using the North American Shale Composite values (NASC; Gromet et al., 1984), generally used in the study of Earth surface processes. Finally, Ce (Ce^*_N) and Eu (Eu^*_N) anomalies have been determined by interpolating the normalized values of adjacent REE, using the equations (Noack et al., 2014):

$$Ce^*_N = \frac{2[Ce]_N}{[La]_N + [Pr]_N} \qquad Eu^*_N = \frac{2[Eu]_N}{[Sm]_N + [Gd]_N}$$

3. Results and discussion

3.1. REE geochemistry in the host rocks and AMD of the IPB

The IPB shows high geological variability which may influence the chemical composition of the AMD. In turn, AMD resulting from sulfide oxidation can interact with different types of country rocks such as gossan, sulfides, shales, jaspers, and felsic, intermediate and mafic volcanic rocks, and inherit their REE fingerprint by dissolution and/or leaching. Table 1 shows a summary of the REE chemical data for the rocks collected in this work and those available in the literature for the IPB. As can be seen from the samples taken in this study, volcanic rocks have the highest concentration of ΣREE, especially those of felsic composition, with an average concentration close to 300 mg/kg. Intermediate and mafic rocks have almost 235 and 155 mg/kg on average, respectively. High concentrations are also present in shales (or sandstones), with more than 240 mg/kg of ΣREE on average. On the other hand, gossan, jaspers and massive sulfides present low ΣREE values (56, 34 and 15 mg/kg, respectively) in comparison with the previous rocks, although disseminated sulfides may present values close to their enclosing host rocks, particularly in rocks of the felsic series and shales. These data agree with the general behavior of the IPB, where the volcanic series (especially felsic) and the shales are the rocks with the highest ΣREE concentrations (average close to 160 and 180 mg/kg, respectively) (Table 1).

Considering the NASC-normalized average values of LREE, MREE and HREE in the rocks shown in Table 1, significant differences in REE patterns can be observed (Fig. 3, Fig. S1). Shales present an almost flat pattern, with a slight enrichment in LREE. Regarding the volcanic rocks, a depletion in LREE is observed, accentuated toward the most mafic

Table 1
REE concentration (mg/kg) in the rocks of this work and in the whole IPB (from literature). Max: maximun, Min: minimun, N: sample size, SD: standard deviation.

		This work				Whole IPB						
Rock Type		N	Min	Max	Mean	N	Min	Max	Mean	Median	SD	References
Gossan		1	-	-	56.3	27	8.0	409.9	86.3	61.6	82.4	12, 15
Sulfides	Massive	1	-	-	15.5	14	1.9	73.3	32.2	31.8	26.6	8, 12
	Disseminate	2	58.6	186.7	122.6	18	12.6	265.5	168.2	163.9	66.0	14, 19
Shales		9	183.8	285.2	244.5	77	50.7	384.6	178.8	170.5	57.5	8, 11, 13, 14, 15, 17, 18, 19
Jaspers		3	6.5	79.1	33.9	22	4.3	133.2	32.4	11.7	34.4	2, 13
Felsic volcanics		11	154.8	800.6	298.6	218	62.0	375.4	162.1	146.5	58.5	1, 3, 4, 5, 6, 7, 9, 10, 13, 16, 20
Intermediate volcanics		2	224.5	244.8	234.7	47	54.7	185.3	109.3	103.9	28.6	3, 5, 9, 10
Mafic volcanics		1	-	-	154.9	83	32.1	212.3	87.3	81.7	32.5	1, 3, 4, 5, 7, 9, 14

References: [1]Almodóvar et al., 1997; [2]Leistel et al., 1997a; [3]Mitjavila et al., 1997; [4]Grimes and Kropschot, 1998; [5]IGME, 1999; [6]Donaire et al., 2002, 2020; [7]Ruiz et al., 2002; [8]Rosa et al., 2004, 2006; [9]Boulter et al., 2004; [10]Capitán, 2006; [11]Barrett et al., 2008; [12]Da silva et al., 2009; [13]Pérez-López et al., 2010; [14]Valenzuela et al., 2011; [15]Jorge et al., 2013; [16]Luz et al., 2019, 2020; [17]Marques et al., 2020.

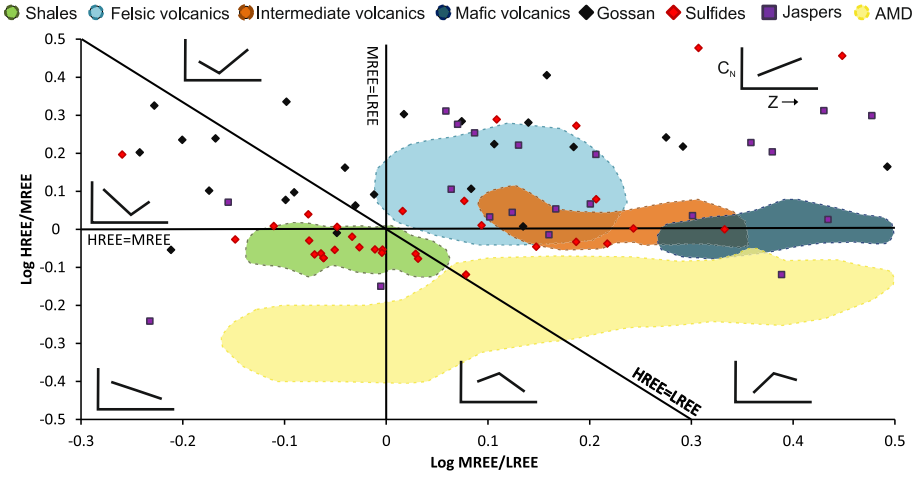

Fig. 3. Stolpe plot of rock samples and AMD from the IPB (data from this study and from the literature. See Table 1 for literature references) according to their average relative content of LREE, MREE and HREE normalized to NASC. Ternary plot version is available as an electronic supplement (Fig. S2).

compositions (Fig. 3). In addition, the felsic series present a characteristic negative Eu anomaly that becomes slightly positive toward the mafic series (Fig. S1). The rest of rocks sampled in this study exhibits variable REE patterns. Gossans are slightly enriched in HREE, and often LREE, over MREE, displaying highly variable Eu anomalies (i.e., positive, negative and no Eu anomaly), mostly positive. On the other hand, jaspers have a pattern generally slightly enriched in HREE and impoverishment in LREE with respect to MREE, with negative and slightly negative Eu and Ce anomalies respectively. Most massive sulfides show a HREE-enriched pattern with a slightly positive Eu anomaly. However, in the case of disseminated sulfides, they appear to inherit the enclosing host rock pattern, showing a flat pattern like that of shales.

AMD generally has a REE pattern characterized by an enrichment in MREE and a slight negative Eu anomaly (Verplanck et al., 2001; Da Silva et al., 2009; Pérez-López et al., 2010; Sahoo et al., 2012; Ayora et al., 2016). Although HREE/MREE ratio in AMD is < 1, they can present high variability in the HREE/LREE and MREE/LREE ratios (León et al., 2021). As can be seen in Figs. 3 and S1, the NASC-normalized REE patterns of AMD in this study and the whole IPB do not seem to match with those of the rocks of the IPB. Therefore, in order to determine the source of REE in these AMD leachates, it is necessary to study at a local scale the REE fractionation processes during the water–rock interaction.

3.2. REE geochemistry of rock leachates from the Perrunal and Poderosa mines

As mentioned above, the different lithologies of the IPB, and specifically of the Poderosa and Perrunal mines, present variable amounts of REE (Table 1). The incongruent dissolution of these rocks under acidic conditions may lead to the release of REE, as can be seen in the results of the leaching tests (Table 2). The highest concentrations of REE released by H_2SO_4 leaching (0.025 M) in the batch experiments are observed in felsic volcanic rocks, shales, intermediate, and mafic volcanic rocks, with concentrations of REE extracted by leachates between 3 and 50, 3–34, 26–32 and 22 mg/kg, respectively. This entail that the leaching mobilized up to 21, 18, 13 and 14 % with respect to the initial REE content of the rock, respectively. Jaspers have similar release percentages, reaching values of 15 %, although their leachates have a very low extracted REE content (average of 2.3 mg/kg), due to the low concentration of REE in the source rock. Finally, sulfides and gossan show very low release percentages and leached concentrations, both below 3.6 % and 2.1 mg/kg rock, respectively. Thus, according to their low release under acidic conditions, gossan, sulfides and jaspers appear to be limited REE contributors to the AMD geochemistry. On the other hand, the highest concentration of sulfuric acid (0.05 M) used in the batch tests results in an increase in the release of REE by 30 and 40 % on average with respect to the leaching with 0.025 M concentration for the rocks of Perrunal and Poderosa, respectively. Meanwhile, the previous step of leaching with ammonium acetate released insignificant amounts of REE, below 1.5 % of the bulk rock for most samples.

It is remarkable that no notable changes are observed in the values of Ce and Eu anomalies for the leachates (0.25 and 0.5 M H_2SO_4) with respect to the bulk rock for most of the samples (Fig S3). This seems to indicate that, during the water–rock interaction, the AMD inherits the Eu and Ce anomalies, and therefore these values could be used as geochemical tracers for potential sources of REE in the leachates. In this sense, the Ce anomaly (Fig. 4A) does not clearly determine the possible REE sources, because the variability of this parameter, both in the rocks of the IPB and in the AMD is not very wide. Thus, all types of rocks show small anomalies, with most groups slightly tending towards the negative anomaly range. It is noteworthy that most of the samples taken in this study coincide with the range observed in the IPB (Fig. 4A). However, since some of the shales or sandstones of the IPB may present resedimented volcanoclastic components (Leistel et al., 1997b; Sáez et al., 1999), shales of this study present slightly negative values with respect to the data observed in the IPB (Fig. 4A), resembling more the range of the volcanic felsic rocks. Finally, AMD from the Perrunal and Poderosa areas also show slightly negative Ce anomalies (Fig. 4A).

Unlike the Ce anomalies, the Eu anomalies show some variability and could provide more information about the source of REEs in AMD. The AMD in the IPB presents generally negative Eu anomalies, as is the case of the Poderosa AMD, although in some cases the absence of anomaly is reported, as occurs in the Perrunal AMD (Fig. 4A). A similar range of Eu anomalies is exhibited by jaspers and felsic volcanic rocks. In the case of

Table 2
ΣREE (mg/kg) of 0.025 M and 0.05 M H_2SO_4 leachates.

	Poderosa mine			Perrunal mine		
Lithology	Sample	0.025 M H_2SO_4	0.05 M H_2SO_4	Sample	0.025 M H_2SO_4	0.05 M H_2SO_4
Gossan	PO-9	1.2	1.4			
Sulfides	PO-8	2.1	2.3	PE-2	0.5	0.6
				PE-3	0.2	0.6
Shales	PO-5	2.7	3.5	PE-5A	24.5	n.a
	PO-6	11.8	13.3	PE-5B	25.2	27.1
	PO-11	4.4	n.a	PE-5C	33.9	n.a
				PE-7	33.6	38.1
				PE-8A	3.8	4.5
				PE-8B	4.5	n.a
Jaspers	PO-4A	1.0	1.4	PE-1	0.9	0.7
	PO-4B	5.2	7.0			
Felsic volcanics	PO-1	20.9	26.8	PE-4	6.4	10.0
	PO-2	15.1	22.9	PE-6B	6.3	6.6
	PO-3	9.4	17.5	PE-9	32.3	38.3
	PO-7	16.4	33.6	PE-11B	49.7	55.2
	PO-10A	20.2	23.4			
	PO-10D	2.8	3.0			
	PO-12	3.1	4.7			
Intermediate volcanics				PE-10B	31.6	n.a
				PE-10C	26.1	n.a
Mafic volcanics			PE-10A	21.8	26.9	

n.a: not analyzed.

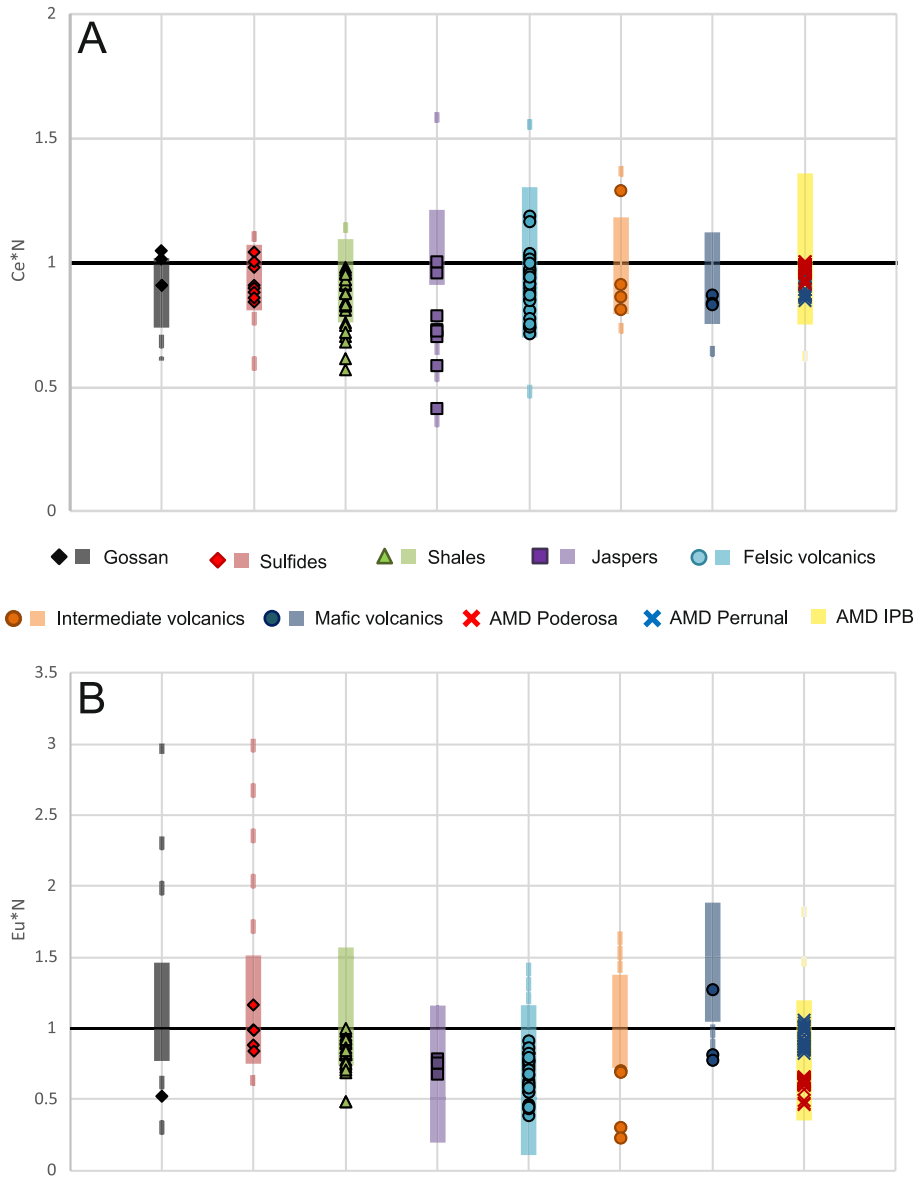

Fig. 4. Ce (A) and Eu (B) anomalies in the different lithologies and AMD of the IPB. The markers represent the samples taken in this work (0.25 and 0.5 M H_2SO_4 and bulk rock), while the background represents the range of the IPB (obtained from literature, whose references can be consulted in Table 1).

mafic volcanic rocks most samples of the IPB display positive anomalies, with intermediate rocks exhibiting Eu anomalies close to + 1. On the other hand, sulfides and gossans present a wide range of variability, from very positive (Eu * N = 3) to negative Eu anomaly values, although most samples are characterized by the absence of anomalies. Finally, the IPB shales are mainly characterized by the absence of a Eu anomaly. However, as in the case of Ce anomalies, the inclusion of volcanosedimentary material in these shales makes some samples exhibit values like those of volcanic rocks. These results seem to focus on felsic and intermediate volcanic rocks, as well as shales with some volcanic components, as the main source of REE in AMD.

Regarding the NASC-normalized REE patterns, it can be observed that the rocks from the Poderosa (Fig. 5A) and Perrunal (Fig. 5B) mines coincide with the fields shown previously for the rocks of the IPB (Fig. 3), except for shales that exhibit patterns similar to those of the felsic rocks as mentioned above. This means that the patterns of the whole rocks differ from the patterns observed in the AMD of both mines, characterized by an enrichment in MREE, and a slight enrichment in LREE with respect to HREE in the Poderosa mine, and the opposite enrichment in the Perrunal mine. Therefore, fractionation processes may occur during acid leaching of these rocks producing these changes in the REE pattern. Indeed, the REE behavior during their release from rock to an acidic medium generates leachates with MREE-enriched patterns like those that appear in AMD. In this sense, the REE source in the AMD of Poderosa mine seems to be related to the dissolution of felsic volcanic rocks, and to a lesser extent to shales and jaspers, which in some cases present a pattern similar to that of felsic rocks (Fig. 5A). On the other hand, the REE source is not so clear as the Perrunal mine as volcanic rocks (both felsic and mafic), shales or jaspers exhibit REE patterns like that of the Perrunal AMD, with slight differences (Fig. 5B). This could indicate that the dissolution of these elements and their enrichment pattern would not occur during the water–rock interaction with a single lithology, but from a combined leaching of various rock types. These hypotheses on the origin of REE in the AMD are consistent with the geology observed in both areas, as has been shown previously, whereas the system of galleries through which the Poderosa AMD runs is located mainly between epiclastic rocks of the felsic series (Fig. 1), the Perrunal area is dominated by shales, but with an important influence from mafic and felsic rocks, and jasper (Fig. 2).

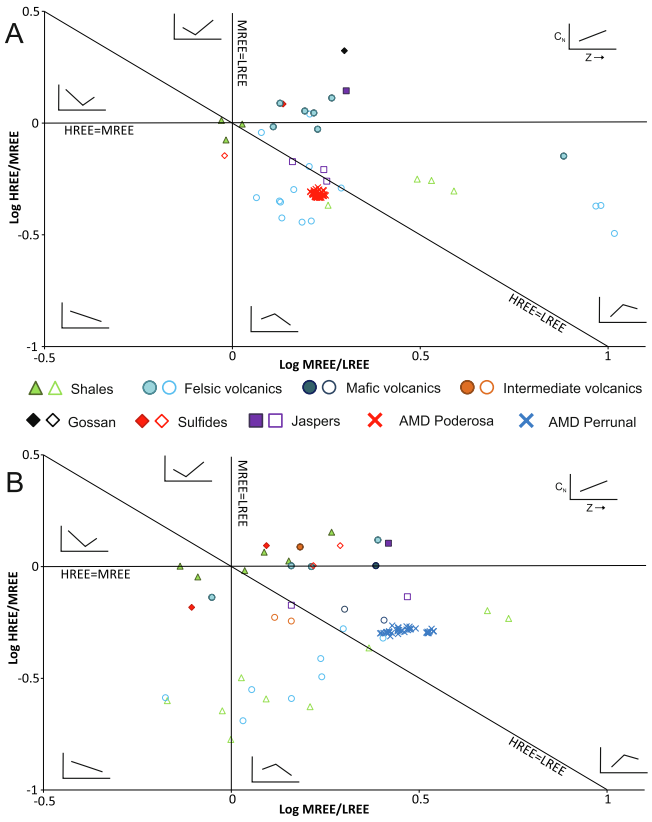

Fig. 5. Stolpe plot of samples from Poderosa (A) and Perrunal mine (B) according to their relative content of LREE, MREE and HREE normalized to NASC. The filled markers represent the whole rock samples, while the empty markers are the samples from rock leaching with sulfuric acid. Ternary plot version is available as an electronic supplement (Fig. S4).

3.3. Mineralogical evidences of the origin of REE in Perrunal and Poderosa mines

As mentioned above, the results of the H_2SO_4 leaching experimentsof the host rocks and sulfides seem to suggest a connection between some lithologies of the host rocks from the Poderosa and the Perrunal mines with the REE patterns found in the AMD. A detailed mineralogical study by FESEM of the rock samples collected in this study has confirmed the existence of a great variety of REE-bearing minerals in the different lithologies of both mines. Significant quantities of LREE-enriched phosphates ((REE)PO_4 enriched in Ce, Nd, La; monazite type) (Fig. 6A,C), which appear systematically in rocks belonging to the felsic volcanic series and the shales, have been observed. On the other hand, HREE-enriched phosphates ((REE)PO_4 enriched in Y, Dy and Er; xenotime type) (Fig. 6A) have been found in most felsic volcanic rocks, while LREE-enriched carbonates ($Ca(REE)_2(CO_3)_3F_2$ enriched in Ce, La, Nd; parisite type) (Fig. 6B) have been observed in carbonate-rich shales from the Perrunal mine. In addition, other minerals such as apatite or zircon have also been detected. However, they may have a minor role as a source of REE due to their slower dissolution kinetics under acid conditions (Ayers and Watson, 1991; Hoshino et al., 2012), and the lower abundance observed with respect to the abovementioned REE-rich phosphates and carbonates. Most of the REE-bearing phosphates and carbonates appear in areas with sericitic alteration, filling holes in the matrix, often accompanied by Fe and/or Ti oxides. Considering the REE pattern of these minerals (Fig. 6D), monazite and parisite have very similar characteristics, with MREE enrichment and a slight HREE depletion with respect to LREE. Within the latter there are two subgroups based on Ca content (Table S1) which are easily identifiable by changes in reflectivity in the FESEM images (Parisites with up to 16–18 % Ca in less reflective zones, and only 0.5–3 % Ca in more reflective zones) (Fig. 6B), however, both groups exhibit the same REE pattern. On the other hand, xenotime displays an enriched pattern in HREE and MREE, with a strong relative depletion in LREE. This variability in the REE patterns within REE-hosting minerals is of paramount importance

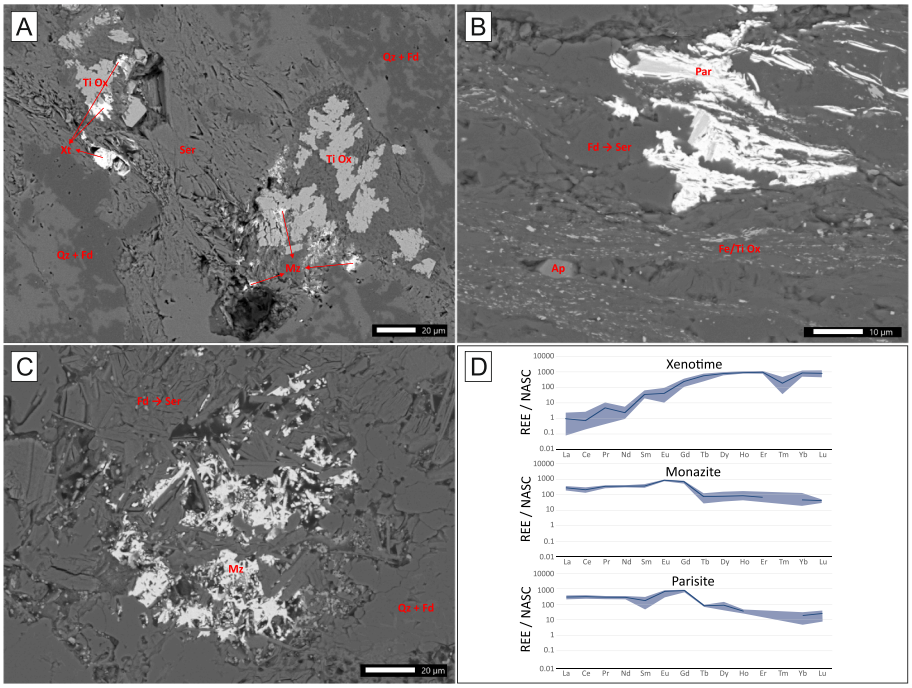

Fig. 6. A: Monazite and xenotime in rhyolite from the felsic volcanic series of the Poderosa mine, B: Parisite in carbonate-rich shales from the Perrunal mine, C: Monazite in felsic volcanic rocks from Poderosa mine, D: Range and average REE patterns in xenotime (n: 17), monazite (n: 14) and parisite (n: 17) from both mines. Chemical data from microprobe mineral analysis are available as an electronic supplement (Table S1). Xt: (REE)PO_4 xenotime type, Par: Ca$(REE)_2(CO_3)_3F_2$ parisite type, Mz: (REE)PO_4 monazite type, Ap: Apatite, Fe/Ti Ox: Fe and/or Ti oxides, Ser: sericite, Fd: feldspar, Qz: quartz.

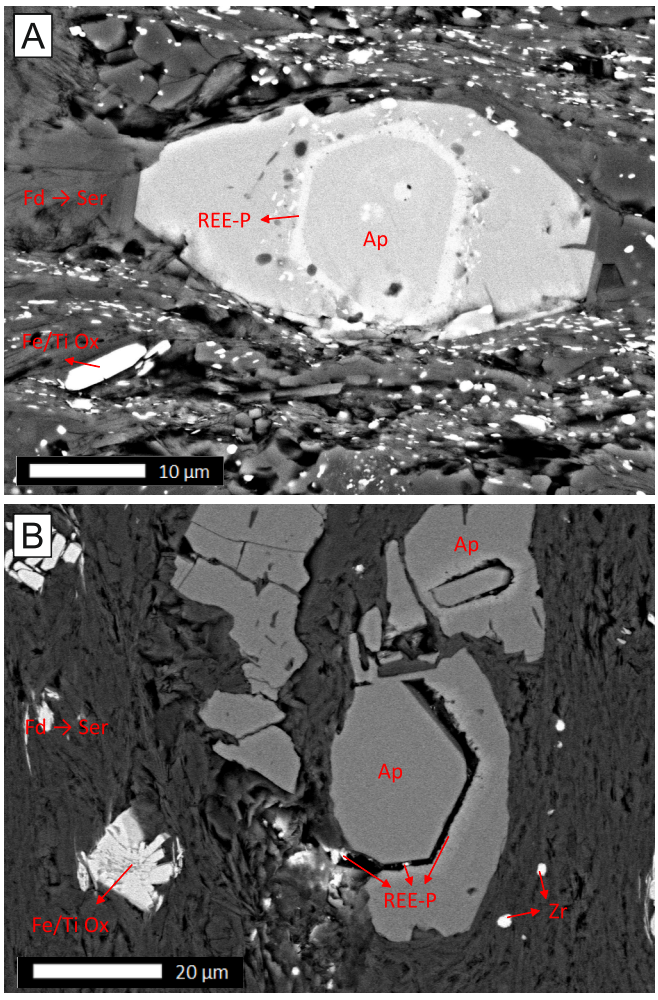

Fig. 7. A: Apatite with LREE phosphate rim in carbonate-rich shales from Perrunal mine, B: Apatite with traces of LREE phosphate rim in felsic volcanic rocks from Perrunal mine. REE-P: (REE)PO_4, Ap: Apatite, Fe/Ti Ox: Fe and/or Ti oxides, Ser: sericite, Fd: feldspar, Zr: zircon.

in the geochemical fingerprint of AMD, since the preferential leaching of any of these minerals (which even coexist in several of the samples studied, see Fig. 6A) could result in the characteristic MREE-enriched REE pattern of AMD, and the relative enrichment in HREE or LREE respectively.

Finally, evidence of this preferential leaching of these REE-rich minerals has been found. Fig. 7 shows the existence of several growth phases in the apatite of the carbonate-rich shales from the Perrunal mine (Fig. 7A), with both growth phases being separated by the formation of an LREE-rich phosphate rim, probably monazite. This REE-rich growth rim around apatite has been described in other context associated to local REE remobilization by hydrothermal fluids (Anenburg et al., 2021).

On the other hand, in rocks from the felsic series of the Perrunal mine (Fig. 7B), the same type of apatite is observed, but the monazite rim appears to have been leached upon acidic conditions, leaving only small remains (<1 µm) and a slight REE enrichment at the edges of the apatite. This mineralogical evidence, that have been observed in several samples, clearly support the hypothesis previously raised that the main source of REE in AMD in the studied area would be readily dissolvable REE-rich phosphates and carbonates.

4. Conclusions

This work has been focused on understanding the origin of REE in the AMD of the IPB, which, according to previous studies, represent an important secondary source of REE with high possibilities of valorization from the economic point of view (León et al., 2021). From a technical point of view, numerous recent studies have focused on the different mechanisms to achieve the recovery of REE from AMD, highlighting the methods based on chemical precipitation, solvent extraction, ion-exchange and adsorption (Mwewa et al., 2022). Despite the possible issues of the different extraction methods, the feasibility of their application in the IPB could be enhanced both by the high concentrations of REE in said leachates (average of 2250 µg/L), and by the environmental requirements of mitigating the pollution generated (León et al., 2021; Mwewa et al., 2022). In this new work, a geological, petrographical, mineralogical and geochemical study of the Poderosa and Perrunal mine rocks (IPB, SW Spain) has made it possible to improve our understanding on the behavior of REE in AMD systems during the interaction of acidic waters with rocks, the potential sources of REE and their fractionation processes. The rocks with the highest REE contents in the IPB are shales and felsic volcanic rocks. Although intermediate and mafic volcanic rocks generally carry somewhat lower concentrations, they may also sporadically have significant amounts of REE, as in the case of the Perrunal mine. On the other hand, gossan, sulfides and jaspers could be excluded as potential sources of REE due to their low concentrations. The patterns presented by these rocks range from flat patterns, to slightly HREE enriched patterns relative to NASC, differing from the patterns observed in the AMD of the IPB, with a characteristic MREE enrichment. Acid leaching experiments (0.25 and 0.5 M H_2SO_4) performed to mimic water–rock interaction in AMD systems have demonstrated the fractionation of REE during the water–rock interaction observed in the field, with MREE-enriched patterns in the leachate from some of these lithologies. Additionally, it has been observed that, during this interaction, the leachate inherits the Ce and Eu anomalies from the rocks and, therefore, these values can serve as a tracer of the source of REE in AMD. Although Ce anomaly values in the case of the IPB do not offer much information due to their low variability in these rocks, the Eu anomaly could help to determine the possible sources of REE. In this sense, the Eu anomalies and the patterns observed in the H_2SO_4 leachates indicate that REE in Poderosa AMD are mainly released from felsic volcanic rocks, while the incongruent dissolution of various lithologies may be the REE source in the AMD of Perrunal mine. Finally, a detailed petrographic examination of the host rocks collected in both study areas documented the existence of REE-rich minerals (i.e., monazite, xenotime and parasite type phases), characterized by different ratios of LREE/HREE. The preferential leaching of these HREE or LREE-enriched minerals, observed by FESEM, may be the responsible of the asymmetry in REE patterns (enriched in HREE over LREE or the opposite) observed in the typical MREE enriched patterns of AMD.

Declaration of Competing Interest

The authors declare that they have no known competing financial interests or personal relationships that could have appeared to influence the work reported in this paper.

Data availability

Data will be made available on request.

Acknowledgements

This work was supported by the Spanish Ministry of Economy and Competitiveness through the research project TRAMPA (MINECO; PID2020-119196RB-C21). Funding for open access charge: Universidad de Huelva / CBUA. We would also like to thank Dr. Franco Pirajno

(Editor-in-Chief), Dr. José María González-Jiménez (Managing Editor), Guest Editor reviewer and anonymous reviewer for the support and suggestions that significantly improved the quality of the original paper.

Appendix A. Supplementary data

Supplementary data to this article can be found online at https://doi.org/10.1016/j.oregeorev.2023.105336. These data include Google maps of the most important areas described in this article.

References

Akcil, A., Koldas, S., 2006. Acid mine drainage (AMD): causes, treatment and case studies. J. Clean. Prod. 14 (12–13), 1139–1145. https://doi.org/10.1016/j.jclepro.2004.09.006.

Almodóvar, G.R., Sáez, R., Pons, J.M., Maestre, A., Toscano, M., Pascual, E., 1997. Geology and genesis of the Aznalcóllar massive sulphide deposits, Iberian Pyrite Belt Spain. Miner. Depos. 33 (1), 111–136. https://doi.org/10.1007/s001260050136.

Almodóvar, G.R., Yesares, L., Sáez, R., Toscano, M., González, F., Pons, J.M., 2019. Massive sulfide ores in the Iberian Pyrite Belt: Mineralogical and textural evolution. Minerals 9 (11), 653. https://doi.org/10.3390/min9110653.

Anenburg, M., Broom-Fendley, S., Chen, W., 2021. Formation of rare earth deposits in carbonatites. Elements Int. Mag. Mineral. Geochem. Petrol. 17 (5), 327–332. https://doi.org/10.2138/gselements.17.5.327.

Åström, M., 2001. Abundance and fractionation patterns of rare earth elements in streams affected by acid sulphate soils. Chem. Geol. 175 (3–4), 249–258. https://doi.org/10.1016/S0009-2541(00)00294-1.

Åström, M., Corin, N., 2003. Distribution of rare earth elements in anionic, cationic and particulate fractions in boreal humus-rich streams affected by acid sulphate soils. Water Res. 37 (2), 273–280. https://doi.org/10.1016/S0043-1354(02)00274-9.

Ayers, J.C., Watson, E.B., 1991. Solubility of apatite, monazite, zircon, and rutile in supercritical aqueous fluids with implications for subduction zone geochemistry. Philos. Trans. R. Soc. Lond. Ser. A: Phys. Eng. Sci. 335 (1638), 365–375. https://doi.org/10.1098/rsta.1991.0052.

Ayora, C., Macías, F., Torres, E., Lozano, A., Carrero, S., Nieto, J.M., Castillo-Michel, H., 2016. Recovery of rare earth elements and yttrium from passive-remediation systems of acid mine drainage. Environ. Sci. Technol. 50 (15), 8255–8262. https://doi.org/10.1021/acs.est.6b02084.

Barrett, T.J., Dawson, G.L., MacLean, W.H., 2008. Volcanic stratigraphy, alteration, and sea-floor setting of the Paleozoic Feitais massive sulfide deposit, Aljustrel, Portugal. Econ. Geol. 103 (1), 215–239. https://doi.org/10.2113/gsecongeo.103.1.215.

Binnemans, K., Jones, P.T., Blanpain, B., Van Gerven, T., Yang, Y., Walton, A., Buchert, M., 2013. Recycling of rare earths: a critical review. J. Clean. Prod. 51, 1–22. https://doi.org/10.1016/j.jclepro.2012.12.037.

Boulter, C.A., Hopkinson, L.J., Ineson, M.G., Brockwell, J.S., 2004. Provenance and geochemistry of sedimentary components in the Volcano-Sedimentary Complex, Iberian Pyrite Belt: discrimination between the sill–sediment-complex and volcanic-pile models. J. Geol. Soc. London 161 (1), 103–115. https://doi.org/10.1144/0016-764902-159.

Cánovas, C.R., Macías, F., Pérez-López, R., 2016. Metal and acidity fluxes controlled by precipitation/dissolution cycles of sulfate salts in an anthropogenic mine aquifer. J. Contam. Hydrol. 188, 29–43. https://doi.org/10.1016/j.jconhyd.2016.02.005.

Cánovas, C.R., Macías, F., Olías, M., 2018. Hydrogeochemical behavior of an anthropogenic mine aquifer: Implications for potential remediation measures. Sci. Total Environ. 636, 85–93. https://doi.org/10.1016/j.scitotenv.2018.04.270.

Capitán, M. Á. (2006). Mineralogía y geoquímica de la alteración superficial de sulfuros masivos en la Faja Pirítica Ibérica (Doctoral dissertation, Universidad de Huelva).

Coppin, F., Berger, G., Bauer, A., Castet, S., Loubet, M., 2002. Sorption of lanthanides on smectite and kaolinite. Chem. Geol. 182 (1), 57–68. https://doi.org/10.1016/S0009-2541(01)00283-2.

Da Silva, E.F., Bobos, I., Matos, J.X., Patinha, C., Reis, A.P., Fonseca, E.C., 2009. Mineralogy and geochemistry of trace metals and REE in volcanic massive sulfide host rocks, stream sediments, stream waters and acid mine drainage from the Lousal mine area (Iberian Pyrite Belt, Portugal). Appl. Geochem. 24 (3), 383–401. https://doi.org/10.1016/j.apgeochem.2008.12.001.

Donaire, T., Sáez, R., Pascual, E., 2002. Rhyolitic globular peperites from the Aznalcóllar mining district (Iberian Pyrite Belt, Spain): physical and chemical controls. J. Volcanol. Geoth. Res. 114 (1–2), 119–128. https://doi.org/10.1016/S0377-0273(01)00287-6.

Donaire, T., Pascual, E., Saez, R., Pin, C., Hamilton, M.A., Toscano, M., 2020. Geochemical and Nd isotopic signature of felsic volcanic rocks as a proxy of volcanic-hosted massive sulphide deposits in the Iberian Pyrite Belt (SW, Spain): The Paymogo Volcano-Sedimentary Alignment. Ore Geol. Rev. 120, 103408 https://doi.org/10.1016/j.oregeorev.2020.103408.

Gammons, C.H., Wood, S.A., Nimick, D.A., 2005. Diel behavior of rare earth elements in a mountain stream with acidic to neutral pH. Geochim. Cosmochim. Acta 69 (15), 3747–3758. https://doi.org/10.1016/j.gca.2005.03.019.

Gonzalo y Tarín, J., 1888. Descripción física, geológica y minera de la provincia de Huelva. Memorias de la Comisión del Mapa Geológico de España. Tomo II (Madrid. 660 pp.). 10.21701/bolgeomin.128.1.006.

Grawunder, A., Merten, D., Büchel, G., 2014. Origin of middle rare earth element enrichment in acid mine drainage-impacted areas. Environ. Sci. Pollut. Res. 21 (11), 6812–6823. https://doi.org/10.1007/s11356-013-2107-x.

Grimes, D. J., & Kropschot, S. J. (Eds.). (1998). Geochemical studies of rare earth elements in the Portuguese Pyrite Belt, and geologic and geochemical controls on gold distribution (No. 1596). US Government Printing Office. 10.3133/pp1596.

Gromet, L.P., Haskin, L.A., Korotev, R.L., Dymek, R.F., 1984. The "North American shale composite": Its compilation, major and trace element characteristics. Geochim. Cosmochim. Acta 48 (12), 2469–2482. https://doi.org/10.1016/0016-7037(84)90298-9.

Hatch, G.P., 2012. Dynamics in the global market for rare earths. Elements 8 (5), 341–346. https://doi.org/10.2113/gselements.8.5.341.

Hedin, B.C., Hedin, R.S., Capo, R.C., Stewart, B.W., 2020. Critical metal recovery potential of Appalachian acid mine drainage treatment solids. Int. J. Coal Geol. 231, 103610 https://doi.org/10.1016/j.coal.2020.103610.

Hoshino, M., Watanabe, Y., Sanematsu, K., Kon, Y., Shimizu, M., 2012. Characteristics of zircon suitable for REE extraction. Int. J. Miner. Process. 102, 130–135. https://doi.org/10.1016/j.minpro.2011.11.006.

IGME (1999). Investigación geológica y cartografía básica en la Faja Pirítica y áreas aledañas. Instituto Tecnológico Geominero de España.

Johannesson, K.H., Zhou, X., 1999. Origin of middle rare earth element enrichments in acid waters of a Canadian High Arctic lake. Geochim. Cosmochim. Acta 63 (1), 153–165. https://doi.org/10.1016/S0016-7037(98)00291-9.

Johnson, D.B., Hallberg, K.B., 2005. Acid mine drainage remediation options: a review. Sci. Total Environ. 338 (1–2), 3–14. https://doi.org/10.1016/j.scitotenv.2004.09.002.

Jorge, R.C.G.S., Fernandes, P., Rodrigues, B., Pereira, Z., Oliveira, J.T., 2013. Geochemistry and provenance of the Carboniferous Baixo Alentejo Flysch Group, South Portuguese Zone. Sed. Geol. 284, 133–148. https://doi.org/10.1016/j.sedgeo.2012.12.005.

Leistel, J.M., Marcoux, E., Deschamps, Y., 1997a. Chert in the Iberian pyrite belt. Miner. Deposita 33 (1), 59–81. https://doi.org/10.1007/s001260050133.

Leistel, J.M., Marcoux, E., Thiéblemont, D., Quesada, C., Sánchez, A., Almodóvar, G.R., Saez, R.J.M.D., 1997b. The volcanic-hosted massive sulphide deposits of the Iberian Pyrite Belt Review and preface to the Thematic Issue. Miner. Depos. 33 (1), 2–30. https://doi.org/10.1007/s001260050130.

León, R., Macías, F., Cánovas, C.R., Pérez-López, R., Ayora, C., Nieto, J.M., Olías, M., 2021. Mine waters as a secondary source of rare earth elements worldwide: The case of the Iberian Pyrite Belt. J. Geochem. Explor. 224, 106742 https://doi.org/10.1016/j.gexplo.2021.106742.

Leybourne, M.I., Cousens, B.L., 2005. In: Rare Earth Elements (REE) aNd Nd aNd Sr Isotopes in GrouNdwater aNd SuspeNded Sediments From the Bathurst Mining Camp, New Brunswick: Water-rock Reactions aNd Elemental Fractionation. Springer, Dordrecht, pp. 253–293. https://doi.org/10.1007/1-4020-3234-X_10.

Leybourne, M.I., Goodfellow, W.D., Boyle, D.R., Hall, G.M., 2000. Rapid development of negative Ce anomalies in surface waters and contrasting REE patterns in groundwaters associated with Zn–Pb massive sulphide deposits. Appl. Geochem. 15 (6), 695–723. https://doi.org/10.1016/S0883-2927(99)00096-7.

Liu, H., Guo, H., Pourret, O., Liu, M., Wang, Z., Zhang, W., Gao, B., Sun, Z., Laine, P., 2022. Geochemical signatures of rare earth elements and yttrium exploited by acid solution mining around an ion-adsorption type deposit: Role of source control and potential for recovery. Sci. Total Environ. 804, 150241 https://doi.org/10.1016/j.scitotenv.2021.150241.

Lozano, A., Ayora, C., Fernández-Martínez, A., 2019a. Sorption of rare earth elements onto basaluminite: the role of sulfate and pH. Geochim. Cosmochim. Acta 258, 50–62. https://doi.org/10.1016/j.gca.2019.05.016.

Lozano, A., Fernández-Martínez, A., Ayora, C., Di-Tomamaso, D., Poulain, A., Rovezzi, M., Marini, C., 2019b. Solid and aqueous speciation of yttrium in passive remediation systems of acid mine drainage. Environ. Sci. Technol. 53, 11153–11161. https://doi.org/10.1021/acs.est.9b01795.

Lozano, A., Ayora, C., Macias, F., Leon, R., Gimeno, M.J., Auque, L., 2020a. Geochemical behavior of rare earth elements in acid drainages: modeling achievements and limitations. J. Geochem. Explor. 216 https://doi.org/10.1016/j.gexplo.2020.106577.

Lozano, A., Ayora, C., Fernández-Martínez, A., 2020b. Sorption of rare earth elements on schwertmannite and their mobility in acid mine drainage treatments. Appl. Geochem. 113 https://doi.org/10.1016/j.apgeochem.2019.104499.

Lucas, J., Lucas, P., Le Mercier, T., Rollat, A., Davenport, W.G., 2014. Rare earths: science, technology, production and use. Elsevier. https://doi.org/10.1557/mrs.2015.109.

Luz, F., Mateus, A., Figueiras, J., Tassinari, C.C., Ferreira, E., Gonçalves, L., 2019. Recognizing metasedimentary sequences potentially hosting concealed massive sulfide accumulations in the Iberian Pyrite Belt using geochemical fingerprints. Ore Geol. Rev. 107, 973–998. https://doi.org/10.1016/j.oregeorev.2019.03.020.

Luz, F., Mateus, A., Rosa, C., Figueiras, J., 2020. Geochemistry of famennian to visean metapelites from the iberian pyrite belt: implications for provenance, paleo-redox conditions and vectoring to massive sulfide deposits. Nat. Resour. Res. 29, 3613–3652. https://doi.org/10.1007/s11053-020-09686-4.

Macías, F., Pérez-López, R., Caraballo, M.A., Cánovas, C.R., Nieto, J.M., 2017. Management strategies and valorization for waste sludge from active treatment of extremely metal-polluted acid mine drainage: a contribution for sustainable mining. J. Clean. Prod. 141, 1057–1066. https://doi.org/10.1016/j.jclepro.2016.09.181.

Marques, A.F.A., Relvas, J.M., Scott, S.D., Rosa, C., Guillong, M., 2020. Melt inclusions in quartz from felsic volcanic rocks of the Iberian Pyrite Belt: Clues for magmatic ore metal transfer towards VMS-forming systems. Ore Geol. Rev. 126, 103743 https://doi.org/10.1016/j.oregeorev.2020.103743.

Merten, D., Geletneky, J., Bergmann, H., Haferburg, G., Kothe, E., Büchel, G., 2005. Rare earth element patterns: a tool for understanding processes in remediation of acid mine drainage. Geochemistry 65, 97–114. https://doi.org/10.1016/j.chemer.2005.06.002.

Mitjavila, J., Marti, J., Soriano, C., 1997. Magmatic evolution and tectonic setting of the Iberian Pyrite Belt volcanism. J. Petrol. 38 (6), 727–755. https://doi.org/10.1093/petroj/38.6.727.

Möller, P., Bau, M., 1993. Rare-earth patterns with positive cerium anomaly in alkaline waters from Lake Van, Turkey. Earth Planet. Sci. Lett. 117 (3–4), 671–676. https://doi.org/10.1016/0012-821X(93)90110-U.

Moreno, C., 1993. Postvolcanic Paleozoic of the Iberian pyrite belt; an example of basin morphologic control on sediment distribution in a turbidite basin. J. Sediment. Res. 63 (6), 1118–1128. https://doi.org/10.1306/D4267CBC-2B26-11D7-8648000102C1865D.

Moreno Garrido, M.C., Sáez Ramos, R., 1990. Sedimentación marina somera en el devónico del anticlinorio de Puebla de Guzmán. Faja Pirítica Ibérica.

Mwewa, B., Tadie, M., Ndlovu, S., Simate, G.S., Matinde, E., 2022. Recovery of rare earth elements from acid mine drainage: a review of the extraction methods. J. Environ. Chem. Eng. 107704 https://doi.org/10.1016/j.jece.2022.107704.

Noack, C.W., Dzombak, D.A., Karamalidis, A.K., 2014. Rare earth element distributions and trends in natural waters with a focus on groundwater. Environ. Sci. Technol. 48 (8), 4317–4326. https://doi.org/10.1021/es4053895.

Nocete, F., 2006. The first specialised copper industry in the Iberian peninsula: Cabezo Juré (2900–2200 BC). Antiquity 80 (309), 646–657. https://doi.org/10.1017/S0003598X00094102.

Nordstrom, D.K., Blowes, D.W., Ptacek, C.J., 2015. Hydrogeochemistry and microbiology of mine drainage: an update. Appl. Geochem. 57, 3–16. https://doi.org/10.1016/j.apgeochem.2015.02.008.

Olias, M., Ceron, J.C., Fernández, I., De la Rosa, J., 2005. Distribution of rare earth elements in an alluvial aquifer affected by acid mine drainage: the Guadiamar aquifer (SW Spain). Environ. Pollut. 135 (1), 53–64. https://doi.org/10.1016/j.envpol.2004.10.014.

Olías, M., Nieto, J.M., 2015. Background conditions and mining pollution throughout history in the Río Tinto (SW Spain). Environments 2 (3), 295–316. https://doi.org/10.3390/environments2030295.

Pérez-López, R., Delgado, J., Nieto, J.M., Márquez-García, B., 2010. Rare earth element geochemistry of sulphide weathering in the São Domingos mine area (Iberian Pyrite Belt): a proxy for fluid–rock interaction and ancient mining pollution. Chem. Geol. 276 (1–2), 29–40. https://doi.org/10.1016/j.chemgeo.2010.05.018.

Pinedo Vara, I. (1963). Piritas de Huelva. Su historia, minería y aprovechamiento. Summa. Madrid, 1-1003.

Rosa, D.R., Inverno, C.M., Oliveira, V.M., Rosa, C.J., 2004. Geochemistry of volcanic rocks, Albernoa area, Iberian pyrite belt, Portugal. Int. Geol. Rev. 46 (4), 366–383. https://doi.org/10.2747/0020-6814.46.4.366.

Rosa, D.R., Inverno, C.M., Oliveira, V.M., Rosa, C.J., 2006. Geochemistry and geothermometry of volcanic rocks from Serra Branca, Iberian pyrite belt, Portugal. Gondwana Res. 10 (3–4), 328–339. https://doi.org/10.1016/j.gr.2006.03.008.

Ruiz, C., Arribas, A., Arribas Jr, A., 2002. Mineralogy and geochemistry of the Masa Valverde blind massive sulphide deposit, Iberian Pyrite Belt (Spain). Ore Geol. Rev. 19 (1–2), 1–22. https://doi.org/10.1016/S0169-1368(01)00037-3.

Sáez, R., Pascual, E., Toscano, M., Almodóvar, G.R., 1999. The Iberian type of volcano-sedimentary massive sulphide deposits. Miner. Depos. 34 (5), 549–570. https://doi.org/10.1007/s001260050220.

Sahoo, P.K., Tripathy, S., Equeenuddin, S.M., Panigrahi, M.K., 2012. Geochemical characteristics of coal mine discharge vis-à-vis behavior of rare earth elements at Jaintia Hills coalfield, northeastern India. J. Geochem. Explor. 112, 235–243. https://doi.org/10.1016/j.gexplo.2011.09.001.

Serrano, M.J.G., Sanz, L.F.A., Nordstrom, D.K., 2000. REE speciation in low-temperature acidic waters and the competitive effects of aluminum. Chem. Geol. 165 (3–4), 167–180. https://doi.org/10.1016/S0009-2541(99)00166-7.

Sholkovitz, E.R., 1995. The aquatic chemistry of rare earth elements in rivers and estuaries. Aquat. Geochem. 1 (1), 1–34. https://doi.org/10.1007/BF01025229.

Stewart, B.W., Capo, R.C., Chadwick, O.A., 2001. Effects of rainfall on weathering rate, base cation provenance, and Sr isotope composition of Hawaiian soils. Geochim. Cosmochim. Acta 65 (7), 1087–1099. https://doi.org/10.1016/S0016-7037(00)00614-1.

Stewart, B.W., Capo, R.C., Hedin, B.C., Hedin, R.S., 2017. Rare earth element resources in coal mine drainage and treatment precipitates in the Appalachian Basin, USA. Int. J. Coal Geol. 169, 28–39. https://doi.org/10.1016/j.coal.2016.11.002.

Sun, H., Zhao, F., Zhang, M., Li, J., 2012. Behavior of rare earth elements in acid coal mine drainage in Shanxi Province, China. Environ. Earth Sci. 67 (1), 205–213. https://doi.org/10.1007/s12665-011-1497-7.

Tang, J., Johannesson, K.H., 2003. Speciation of rare earth elements in natural terrestrial waters: assessing the role of dissolved organic matter from the modeling approach. Geochim. Cosmochim. Acta 67 (13), 2321–2339. https://doi.org/10.1016/S0016-7037(02)01413-8.

Valenzuela, A., Donaire, T., Pin, C., Toscano, M., Hamilton, M.A., Pascual, E., 2011. Geochemistry and U-Pb dating of felsic volcanic rocks in the Riotinto-Nerva unit, Iberian Pyrite Belt, Spain: crustal thinning, progressive crustal melting and massive sulphide genesis. J. Geol. Soc. London 168 (3), 717–732. https://doi.org/10.1144/0016-76492010-081.

Vass, C.R., Noble, A., Ziemkiewicz, P.F., 2019. The occurrence and concentration of rare earth elements in acid mine drainage and treatment by-products: part 1—initial survey of the Northern Appalachian Coal Basin. Min. Metall. Explor. 36 (5), 903–916. https://doi.org/10.1007/s42461-019-0097-z.

Verplanck, P.L., Antweiler, R.C., Nordstrom, D.K., Taylor, H.E., 2001. Standard reference water samples for rare earth element determinations. Appl. Geochem. 16 (2), 231–244. https://doi.org/10.1016/S0883-2927(00)00030-5.

Verplanck, P.L., Nordstrom, D.K., Taylor, H.E., Kimball, B.A., 2004. Rare earth element partitioning between hydrous ferric oxides and acid mine water during iron oxidation. Appl. Geochem. 19 (8), 1339–1354. https://doi.org/10.1016/j.apgeochem.2004.01.016.

Wallrich, I.L., Stewart, B.W., Capo, R.C., Hedin, B.C., Phan, T.T., 2020. Neodymium isotopes track sources of rare earth elements in acidic mine waters. Geochim. Cosmochim. Acta 269, 465–483. https://doi.org/10.1016/j.gca.2019.10.044.

Welch, S.A., Christy, A.G., Isaacson, L., Kirste, D., 2009. Mineralogical control of rare earth elements in acid sulfate soils. Geochim. Cosmochim. Acta 73 (1), 44–64. https://doi.org/10.1016/j.gca.2008.10.017.

Worrall, F., Pearson, D.G., 2001. The development of acidic groundwaters in coal-bearing strata: Part I Rare earth element fingerprinting. Appl. Geochem. 16 (13), 1465–1480. https://doi.org/10.1016/S0883-2927(01)00018-X.

Younger, P.L., 1997. The longevity of minewater pollution: a basis for decision-making. Sci. Total Environ. 194, 457–466. https://doi.org/10.1016/S0048-9697(96)05383-1.

Zhang, W., Honaker, R.Q., 2018. Rare earth elements recovery using staged precipitation from a leachate generated from coarse coal refuse. Int. J. Coal Geol. 195, 189–199. https://doi.org/10.1016/j.coal.2018.06.008.

Zhang, W., Honaker, R., 2020. Process development for the recovery of rare earth elements and critical metals from an acid mine leachate. Miner. Eng. 153, 106382 https://doi.org/10.1016/j.mineng.2020.106382.

Zhao, F., Cong, Z., Sun, H., Ren, D., 2007. The geochemistry of rare earth elements (REE) in acid mine drainage from the Sitai coal mine, Shanxi Province, North China. Int. J. Coal Geol. 70 (1–3), 184–192. https://doi.org/10.1016/j.coal.2006.01.009.

Ziemkiewicz, P., He, T., Noble, A., & Liu, X. (2016, March). Recovery of rare earth elements (REEs) from coal mine drainage. In West Virginia Mine Drainage Task Force Symposium: Morgantown, WV, USA.